Eur. Phys. J. C (2015) 75:91
DOI 10.1140/epjc/s10052-015-3310-3

THE EUROPEAN PHYSICAL JOURNAL C

Regular Article - Theoretical Physics

Proposal for resonant detection of relic massive neutrinos

Jeremiah Birrell[a], **Johann Rafelski**

Department of Physics, University of Arizona, Tucson, AZ 85721, USA

Received: 24 November 2014 / Accepted: 8 February 2015 / Published online: 24 February 2015

Abstract We present a novel method for detecting the relic neutrino background that takes advantage of structured quantum degeneracy to amplify the drag force from neutrinos scattering off a detector. Developing this idea, we present a characterization of the present day relic neutrino distribution in an arbitrary frame, including the influence of neutrino mass and neutrino reheating by e^+e^- annihilation. We present explicitly the neutrino velocity and de Broglie wavelength distributions for the case of an Earthbound observer. Considering that relic neutrinos could exhibit quantum liquid features at the present day temperature and density, we discuss the impact of neutrino fluid correlations on the possibility of resonant detection.

1 Introduction

Among the great science and technology challenges of this century is the development of the experimental capability to detect cosmic background neutrinos. To this end, we study the neutrino background as it is expected today, based on the freeze-out condition in the dense early Universe, combined with subsequent free-streaming and redshifting to temperatures below the neutrino mass. In consideration of these results we argue that the present day massive relic neutrino background could form a quantum Fermi liquid state. We present arguments that the correlations inherent in a neutrino quantum Fermi liquid could be exploited in novel detection methods that utilize resonant amplification of relic neutrino drag forces.

This approach is in contrast to prior attempts to find a directly observable signature of the relic neutrinos, which have focused on the magnitude of the mechanical force due to scattering from a massless neutrino background [1–15]. The consensus reached in the literature is that, for an unstructured (relativistic) neutrino gas, such effects are far from the abilities of current detector technology. Aside from elastic scattering there are also inelastic processes–we note the development of the PTOLEMY experiment [16] aiming to observe relic electron neutrino capture by tritium, as originally proposed by Weinberg [17].

In this paper we will first characterize the free-streaming distribution from the perspective of an observer in relative motion under the usual Boltzmann dilute gas assumption, utilizing the physically consistent equation of state from [18]. We will then argue that high degree of degeneracy of the non-equilibrium relic neutrino distribution, together with their temperature $T_\nu \ll m_\nu$, implies the inadequacy of the dilute gas assumption, resulting in a correlated background. This leads us to explore the possibility of the detection of relic neutrinos by resonant amplification of the neutrino–detector interaction.

In our characterization of the cosmic neutrino background (CNB), we will focus on two important physical characteristics, namely the neutrino mass and effective number of neutrinos N_ν. $N_\nu \neq 3$ signals either a yet undiscovered massless particle inventory in the Universe, or as we will assume in this work, a transfer of e^+e^- annihilation entropy into neutrinos resulting in their momentum distribution being 'hotter' than generally accepted [18]. The magnitude of the neutrino freeze-out temperature T_k controls the amount of entropy that is transferred from $e^\pm$ into neutrinos before freeze-out.

A numerical study based on the Boltzmann equation with two body standard model (SM) scattering [19] gives $N_\nu^{\rm th} = 3.046$. N_ν impacts Universe dynamics and recent experimental PLANCK CMB results contain several fits [20] which suggest that $N_\nu \simeq (3.30\text{–}3.62) \pm 0.25$. PLANCK CMB and lensing observations [21] lead to $N_\nu = 3.45 \pm 0.23$.

In consideration of the complexity of low energy neutrino interactions with the dense $e^\pm$ plasma near $T = O(1\text{MeV})$, we treated the freeze-out temperature T_k as a free parameter and obtained the dependence of the free-streaming neutrino distribution on T_k in [18]. In particular, we find that the T_k dependence can be expressed in terms of the measured value

[a] e-mail: jeremey.birrell@gmail.com; jbirrell@email.arizona.edu

N_ν and vice verse. This was done under the assumption of a strictly SM-particle inventory and allowed for a determination of the effect of neutrino mass m_ν^i, and N_ν on the equations of state determining the Universe expansion. A value of $N_\nu \simeq 3.5$ can be interpreted in terms of a delayed neutrino freeze-out during the $e^\pm$ annihilation era. In the following we treat N_ν as a variable model parameter within the general observed experimental range and use the above mentioned relations to characterize our results in terms of N_ν.

There are several available bounds on neutrino masses:

(a) Neutrino energy and pressure components are important before photon freeze-out and thus m_ν impacts Universe dynamics. The analysis of cosmic microwave background (CMB) data alone leads to $\sum_i m_\nu^i < 0.66$ eV ($i = e, \mu, \tau$) and including Baryon Acoustic Oscillation gives $\sum m_\nu < 0.23$ eV [20]. PLANCK CMB with lensing observations [21] lead to $\sum m_\nu = 0.32 \pm 0.081$ eV.
(b) Upper bounds have been placed on the electron neutrino mass in direct laboratory measurements $m_{\bar{\nu}_e} < 2.05$ eV [22,23].

In the subsequent analysis we will focus on the neutrino mass range 0.05–2 eV in order to show that direct measurement sensitivity allows for the exploration of a wide mass range.

In Sect. 2 we introduce the free-streaming massive neutrino distribution. We present our characterization of the neutrino distribution, including the dependence on N_ν and m_ν, in Sect. 3. In Sect. 4 we show that at present day temperatures and densities, the CNB will have properties of a quantum Fermi fluid, including density correlations. With this, we discuss the possibility of detection via resonance with the neutrino dynamical correlation frequency, which we estimate in the Earth frame to be within the range 110–160 MHz.

2 The free-streaming neutrino distribution

The neutrino background and the CMB were in equilibrium until decoupling (called freeze-out) at $T_k \simeq O$ (MeV). In the cosmological setting, for $T < T_k$ the decoupled neutrino spectrum evolves according to the Fermi–Dirac–Einstein–Vlasov (FDEV) free-streaming distribution [7,18,24,25],

$$f(t, p) = \frac{1}{\Upsilon_\nu^{-1} e^{\sqrt{p^2/T_\nu^2 + m_\nu^2/T_k^2}} + 1}. \quad (1)$$

Υ_ν is the fugacity factor, here describing the underpopulation of neutrino phase space that was frozen into the neutrino FDEV distribution in the process of decoupling from the $e^\pm$, γ-QED background plasma. The relation between Υ_ν and T_k is given in Ref. [18]. For $N_\nu \approx 3$, Υ_ν is close to 1, but for delayed freeze-out scenarios, Υ_ν can deviate significantly form 1. Setting $T_k = 0$ and $\Upsilon_\nu = 1$ we obtain the baseline distribution used in [26].

The neutrino effective temperature $T_\nu(t) = T_k\,(a(t_k)/a(t))$ is the scale-shifted freeze-out temperature T_k. Here $a(t)$ is the cosmological scale factor where $\dot{a}(t)/a(t) \equiv H$ is the observable Hubble parameter.

The physical origin of the distribution Eq. (1) is quite simple. At the freeze-out time, when $T = T_k$, Eq. (1) matches the equilibrium distribution. After decoupling, each particle travels through the Universe on a geodesic, free of interactions other than gravity. The effects of gravity are simply the usual redshifting of momentum. This implies that the distribution must be a function of $a(t)p$ only ($1/a(t)$ being the redshift temperature scaling) and so, given the initial condition at $T = T_k$, the necessary form is Eq. (1).

In practice, we will neglect $m_\nu/T_k \lesssim 10^{-7}$. This gives the distribution the same form as that of a massless fermion. In other words, the fact that freeze-out occurred at $T_k \gg m_\nu$ means that the free-streaming distribution carries little information about the mass. However, it is important to recall that we are not dealing with a textbook massless Fermi gas; all dynamical and kinematic observables, such as the energy density, pressure, velocity etc., will involve the neutrino mass. This gives the results for a free-streaming particle a decidedly non-equilibrium nature, despite the familiar forms of some expressions.

An important consequence of the structure of weak interactions is that $T_k \gg m_\nu$, meaning that freeze-out occurs prior to large scale annihilation of neutrinos. This implies that the present day number density of neutrinos is much higher compared to an equilibrium density. This has important implications for the quantum nature of the CNB. We will discuss this further in Sect. 4.

3 Characterizing the neutrino distribution in a moving frame

The neutrino background and the CMB were in equilibrium, mediated by $e^\pm$ plasma, until decoupling. Therefore one surmises that an observer would have the same relative velocity, $v_{\rm rel}$, relative to the relic CNB as with the CMB. Measurements of the CMB dipole anisotropy yield a relative solar system CMB velocity of $v_\oplus = 369.0 \pm 0.9$ km/s [27]. Taking into account the relative orientation of the earth orbital plane and the dipole direction (but neglecting ellipticity of the orbit), the relative velocity is modulated in the range $(-29.2, 29.3)$ km/s [28]. In the following we will write velocities in units of c, though our specific results will be presented in km/s.

By casting the neutrino distribution, Eq. (1), in a relativistically invariant form we can make a transformation to the

rest frame of an observer moving with relative velocity $v_{\rm rel}$ to obtain

$$f(p^\mu) = \frac{1}{\Upsilon_\nu^{-1} e^{\sqrt{(p^\mu U_\mu)^2 - m_\nu^2}/T_\nu} + 1}. \quad (2)$$

The 4-vector characterizing the rest frame of the neutrino FDEV distribution is

$$U^\mu = (\gamma, 0, 0, v_{\rm rel}\gamma), \quad \gamma = 1/\sqrt{1 - v_{\rm rel}^2}, \quad (3)$$

where we have chosen coordinates so that the relative motion is in the z-direction. See [29,31] for further discussion of the effects of the neutrino distribution anisotropy in the Earth frame.

Using Eq. (2), the normalized FDEV velocity distribution for an observer in relative motion is obtained has the form

$$f_v = \frac{g_\nu}{n_\nu 4\pi^2} \int_0^\pi \frac{p^2 {\rm d}p/{\rm d}v \sin(\phi) {\rm d}\phi}{\Upsilon_\nu^{-1} e^{\sqrt{(E - v_{\rm rel} p\cos(\phi))^2 \gamma^2 - m_\nu^2}/T_\nu} + 1},$$
$$p(v) = \frac{m_\nu v}{\sqrt{1 - v^2}}, \qquad \frac{{\rm d}p}{{\rm d}v} = \frac{m_\nu}{(1 - v^2)^{3/2}}. \quad (4)$$

where g_ν is the neutrino degeneracy and n_ν is the number density in the current frame. f_v was obtained by marginalizing over the angular variables, hence the integration over ϕ. The θ integral was performed analytically.

The normalization n_ν depends on N_ν but not on m_ν since decoupling occurred at $T_k \gg m_\nu$. For each neutrino flavor (all flavors are equilibrated by oscillations) we have, per neutrino or antineutrino and at non-relativistic relative velocity,

$$n_\nu = [-0.36\delta N_\nu^2 + 6.7\delta N_\nu + 56]\ {\rm cm}^{-3} \quad (5)$$

($\delta N_\nu \equiv N_\nu - 3$). This is obtained by integrating the distribution Eq. (2) and using the relations between Υ_ν, T_ν, and N_ν derived in Ref. [18].

We show f_v in Fig. 1 for several values of the neutrino mass, $v_{\rm rel} = 369$ km/s, and $N_\nu = 3.046$ (solid lines) and $N_\nu = 3.62$ (dashed lines). As discussed above, the former corresponds to standard model neutrino decoupling, while the latter corresponds to a delayed freeze-out scenario. From Ref. [18], the respective fugacities are $\Upsilon_\nu = 0.97$, $\Upsilon_\nu = 0.71$. As expected, the lighter the neutrino, the more f_v is weighted toward higher velocities with the velocity becoming visibly peaked about $v_{\rm rel}$ for $m_\nu = 2$ eV.

A similar procedure produces the normalized FDEV energy distribution f_E. In Eq. (4) we replace ${\rm d}p/{\rm d}v \to {\rm d}p/{\rm d}E$ where it is understood that

$$p(E) = \sqrt{E^2 - m_\nu^2}, \qquad \frac{{\rm d}p}{{\rm d}E} = \frac{E}{p}. \quad (6)$$

We show f_E in Fig. 2 for several values of the neutrino mass, $v_{\rm rel} = 369$ km/s, and $N_\nu = 3.046$ (solid lines) and $N_\nu = 3.62$ (dashed lines). The width of the FDEV energy distribution is

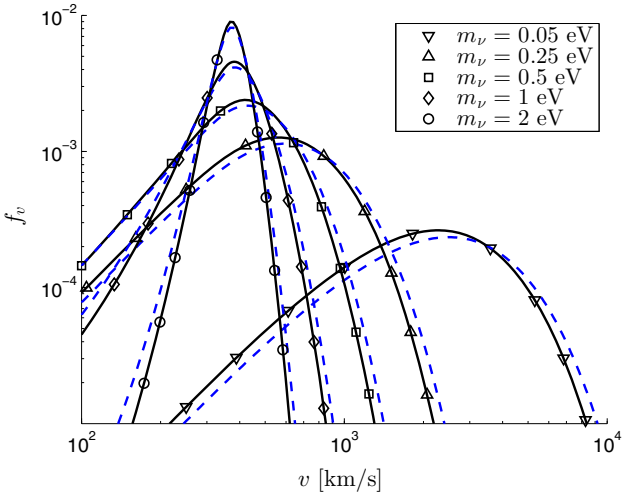

Fig. 1 Normalized neutrino FDEV velocity distribution in the Earth frame. We show the distribution for $N_\nu = 3.046$ (*solid lines*) and $N_\nu = 3.62$ (*dashed lines*)

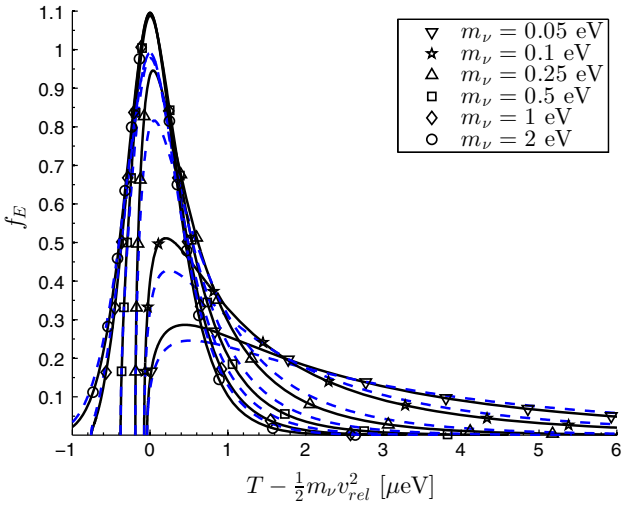

Fig. 2 Neutrino FDEV energy distribution in the Earth frame. We show the distribution for $N_\nu = 3.046$ (*solid lines*) and $N_\nu = 3.62$ (*dashed lines*)

on the micro-eV scale and the kinetic energy $T = E - m_\nu$ is peaked about $T = \frac{1}{2}m_\nu v_{\rm rel}^2$, implying that the relative velocity between the Earth and the CMB is the dominant factor for $m_\nu > 0.1$ eV.

By multiplying f_E by the neutrino velocity and number density for a single neutrino flavor (without antineutrinos) we obtain the particle flux density,

$$\frac{{\rm d}J}{{\rm d}E} \equiv \frac{{\rm d}n}{{\rm d}A{\rm d}t{\rm d}E}, \quad (7)$$

shown in Fig. 3. We show the result for $N_\nu = 3.046$ (solid lines) and $N_\nu = 3.62$ (dashed lines). The flux is normalized in these cases to a local density 56.6 and 60.4 cm^{-3},

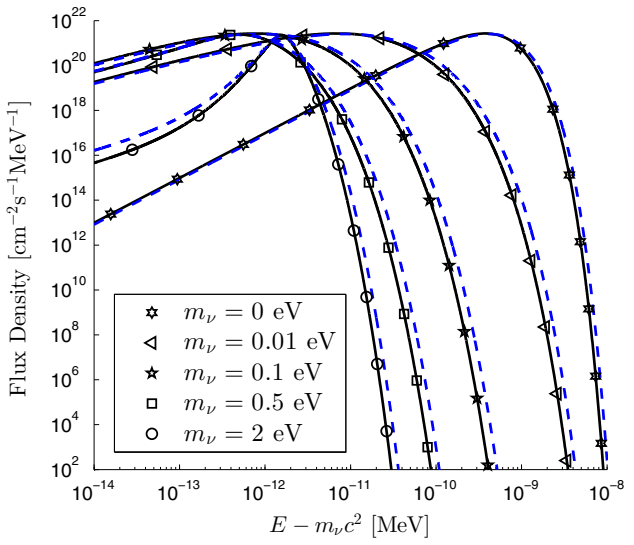

Fig. 3 Neutrino flux density in the Earth frame. We show the result for $N_\nu = 3.046$ (*solid lines*) and $N_\nu = 3.62$ (*dashed lines*)

respectively. The precise neutrino flux in the Earth frame is significant for efforts to detect relic neutrinos, such as the PTOLEMY experiment [16]. The energy dependence of the flux shows a large sensitivity to the mass. However, the maximal fluxes do not vary significantly with m. In fact the maximum values are independent of m when $v_{\rm rel} = 0$, as follows from the fact that $v = p/E = \mathrm{d}E/\mathrm{d}p$. In the Earth frame, where $0 < v_\oplus \ll c$, this translates into only a small variation in the maximal flux.

Using $\lambda = 2\pi/p$ we find in the normalized FDEV de Broglie wavelength distribution

$$f_\lambda = \frac{2\pi g_\nu}{n_\nu \lambda^4} \int_0^\pi \frac{\sin(\phi)\mathrm{d}\phi}{\Upsilon_\nu^{-1} \mathrm{e}^{\sqrt{(E - v_{\rm rel} p\cos(\phi))^2\gamma^2 - m_\nu^2}/T_\nu} + 1} \tag{8}$$

shown in Fig. 4 for $v_{\rm rel} = 369$ km/s and for several values m_ν comparing $N_\nu = 3.046$ with $N_\nu = 3.62$.

4 Neutrinos as a quantum fluid

The prospects for detecting an unstructured relic neutrino background due to neutrino scattering from a detector has been studied by many authors, both the $O(G_F)$ effects debated in [1–3,5,7–9] and the $O(G_F^2)$ force in [6,8,12], and were eventually found to be well beyond the reach of current detection efforts.

Considering the recent establishment of neutrino mass well above the scale of temperature of the neutrino background, a new physics opportunity arises which has not been considered in the earlier efforts. While treating the scattering as a quantum process, all earlier studies modeled the CNB

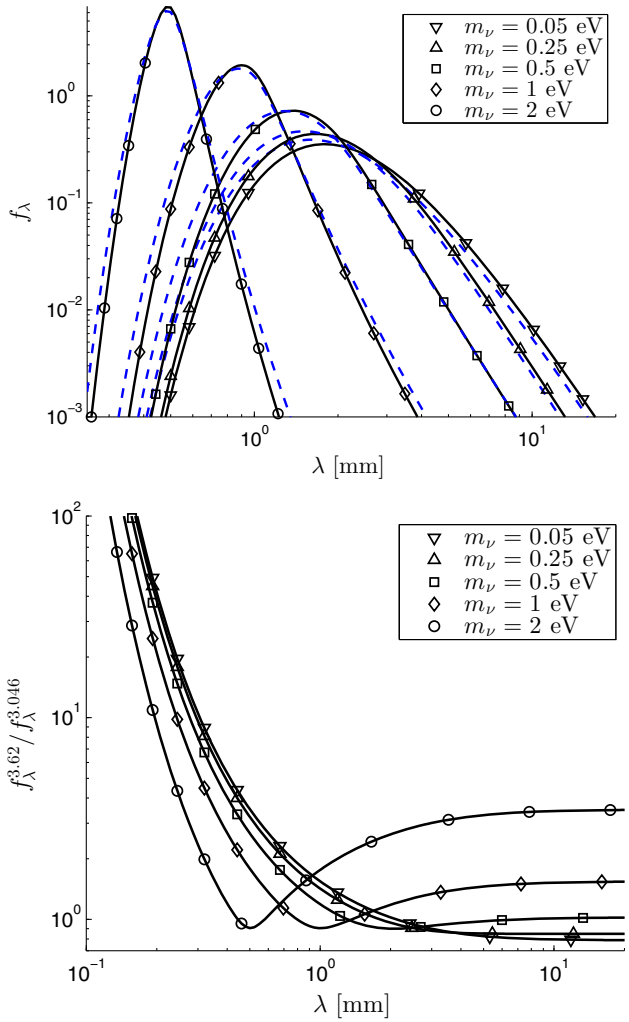

Fig. 4 Neutrino FDEV de Broglie wavelength distribution in the Earth frame. We show in *top panel* the distribution for $N_\nu = 3.046$ (*solid lines*) and $N_\nu = 3.62$ (*dashed lines*) and in *bottom panel* their ratio

distribution as an unstructured particle gas. As a consequence of this assumption, each neutrino impact on a detector is independent of the others. This means that irrespective of the spectrum structure we presented in the previous section, the impact to impact correlation of events in a neutrino detector is a white shot noise spectrum. Hence only the overall strength of the interaction is relevant for neutrino detection.

However, once one accepts that $m_\nu \gg T_\nu$, i.e. that neutrinos become 'cold' in the free-streaming process while the Universe expands and cools, one sees that the CNB neutrinos must form a dense quantum fluid. While we are first to note this in context of neutrino detection, quantum CNB properties have already been recognized in a different context [30].

The expected degeneracy is further enhanced by gravitational accretion. This has been studied previously for a classical particle gas of neutrinos [26,31]. The former found density enhancement by a factor of 1–10 or more for neutrino masses on the scale of 0.1 eV. To quantify the importance of

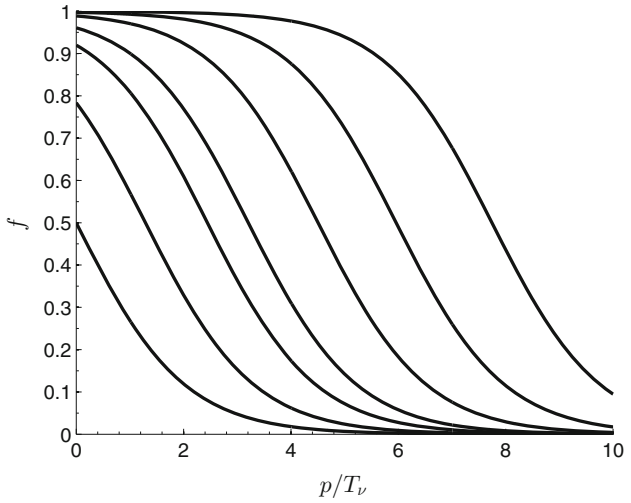

Fig. 5 Neutrino distribution in the CMB frame with chemical potential corresponding to density enhancement by a factor of 1, 2, 5, 10, 25, 50, 100 (*bottom to top*)

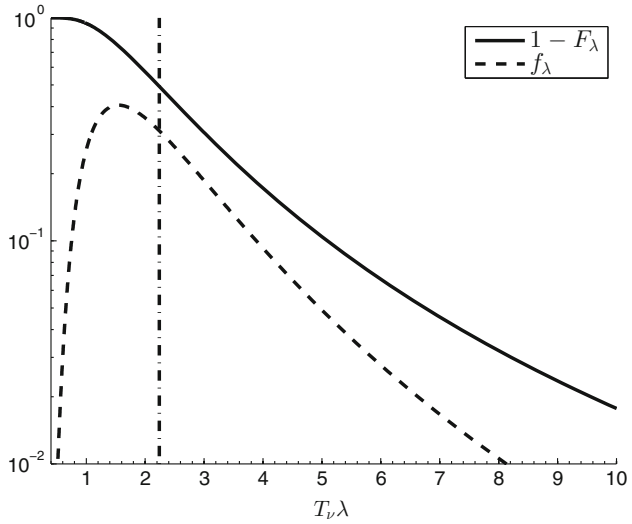

Fig. 6 Neutrino de Broglie wavelength distribution (*dashed line*) and one minus the cumulative distribution (*solid line*), both computed in the CMB frame, with no density enhancement. The *vertical line* shows $T_\nu/n_\nu^{1/3}$, a measure of the characteristic separation between neutrinos of a given flavor

gravitational accretion on the neutrino quantum fluid structure we show in Fig. 5 the neutrino distribution as a function of momentum normalized by temperature and corresponding to a density enhancement factor of 1, 2, 5, 10, 25, 50, 100 (bottom to top). We see in Fig. 5 that the quantum degeneracy increases rapidly and if indeed neutrinos accrete in the expected way, we are today immersed in a nearly degenerate quantum liquid. We return to this point further below.

A precise model of the background neutrino density correlations would require modeling their formation as the Universe cools while it expands and, equally importantly, incorporating the effects of solar system gravitational enhancement in the local quantum fluid distribution as discussed above. These steps are beyond the scope of this initial proposal. However, the presence of correlations in a quantum fluid is a well understood feature within the context of condensed matter physics [32], and we will base our arguments on this analogy–we believe that the pivotal outcome of this circumstance can be captured by considering neutrino impacts on the detector to be strongly correlated, leading to a structured impact spectrum that can be leveraged for resonant detection. We will investigate this now within a simple model.

The importance of quantum effects is recognized in Fig. 6 where we show the neutrino de Broglie wavelength distribution (dashed line) and cumulative distribution (solid line), both computed in the CNB rest frame for $N_\nu = 3.046$. The fact that we study now the neutrino liquid in the rest frame of the relic neutrinos where the distribution is a function of momentum only, see Eq. (2), makes the result independent of neutrino mass.

The vertical line shows the value of $T_\nu L$ where the $L \equiv n_\nu^{-1/3}$, a measure of the average separation between neutrinos. In computing n_ν, the degeneracy must be taken to be equal to one. There is no spin degeneracy as neutrinos (antineutrinos) are left (right) handed, meaning in this context that there is one neutrino state of each flavor. (This is not the place to resolve the well known problem that handedness and helicity are not one and the same thing once neutrinos have a mass.) We consider the density of only a single neutrino flavor at a time and without the corresponding antiparticle, so that we can ascertain the degree to which exclusion principle considerations make this a quantum system. The conversion of one flavor into another (neutrino oscillation) does not affect this constraint as for the present we assume that in equilibrium as many neutrinos oscillate out into another flavor as they oscillate in.

The cumulative distribution in Fig. 6 shows that approximately 50 % of the neutrinos have de Broglie wavelength longer than L, indicating the importance of quantum effects in the homogeneous Universe, without any gravitational accretion. This result is independent of T_ν for $T_\nu < T_k$, as the redshifting of momentum and temperature compensate one another. In other words, the high density nature of the neutrino background in the early Universe, in terms of particles per de Broglie volume, is preserved in the subsequent free-streaming evolution because freeze-out occurs at $T_k \gg m_\nu$. This important insight would be lost if one were to use (incorrectly) a thermal equilibrium neutrino distribution, since massive thermal neutrinos with $m_\nu > T_\nu$ are very dilute.

We now return to consider the effect of density enhancement via gravitational accretion of neutrinos discussed above. Density increase (while maintaining the effective tempera-

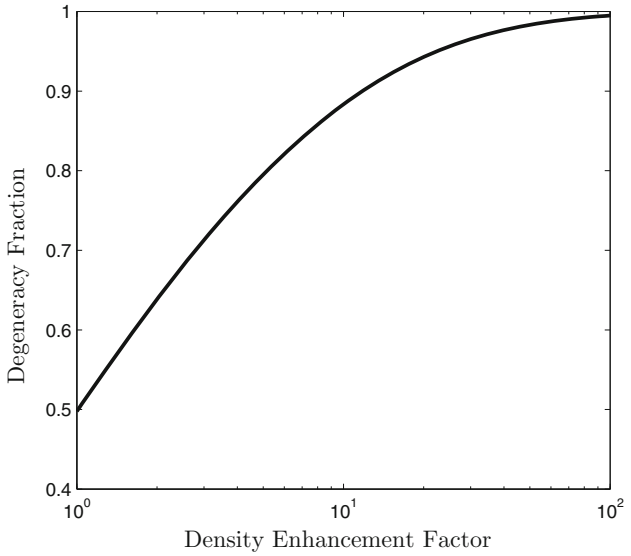

Fig. 7 Fraction of neutrinos whose de Broglie wavelength is longer than the characteristic separation length, see Fig. 6, as a function of the density enhancement factor compared to homogeneous Universe density

ture) leads to a significant increase in degeneracy, and hence to strengthening of the quantum nature of the relic neutrino fluid. We illustrate this in a quantitative fashion in Fig. 7, where we show the fraction of neutrinos whose de Broglie wavelength is longer than the characteristic separation length $T_\nu/n_\nu^{1/3}$, as a function of the density enhancement factor due to accretion. As already noted, on the left we see that about half of neutrinos are degenerate in a homogeneous Universe and this fraction rises to 85 % for a factor of 10 neutrino density enhancement in the galaxy.

5 Neutrinos quantum fluid detection

We turn now to evaluate the experimental opportunity provided by the newly recognized quantum correlations between neutrino impacts. A detailed evaluation of the neutrino shot noise spectrum is beyond the scope of this work. However, much can be learned from a simple model.

First, we observe that neutrino oscillation measurements imply that at least one neutrino species has sufficiently high mass for the corresponding component of the CNB to be very cold, $m_\nu \gg T_\nu$ [22]. The quantum nature of a cold massive fermion liquid will induce correlations in the CNB, even in the absence of interactions, due to Pauli–Fermi exchange effect repulsion [33]. Such correlations will cause the temporal spectrum of neutrinos scattering from a detector to deviate from white noise. We emphasize that we are not assuming that the potential (i.e. the detector) from which the neutrinos scatter is noisy, rather the noise is provided by the stochastic process consisting of neutrino impacts on the detector. For our discussion to be meaningful it is necessary that the detector is cooled to sufficiently low temperature so that the thermal noise in the detector does not wash out the signal from correlated neutrino impacts.

We make a crude estimate of the impact correlation by assuming a perfect cubic lattice with side length $L = n_\nu^{-1/3}$. In this case the neutrino impacts are not random and the characteristic frequency for such a lattice is

$$f_{\rm shot} = n_\nu^{1/3} v_{\rm rel} \tag{9}$$

which, as a function of $\delta N_\nu \equiv N_\nu - 3$ and with $v_{\rm rel} = 369$ km/s, is given by the following fit:

$$f_{\rm shot} = (-0.43\delta N_\nu^2 + 5.6\delta N_\nu + 140)\frac{v_{\rm rel}}{369\ {\rm km/s}}\ {\rm MHz}. \tag{10}$$

The annual Earth orbital velocity and daily rotation velocity produce a shifted frequency response as a function of $\delta v_{\rm rel} \equiv v_{\rm rel} - v_\oplus$ in the approximate range ± 30 km/s, and is an important signature that distinguishes a neutrino signal from other noise sources. This modulation, together with $0 \le \delta N_\nu \le 0.8$, gives $129 \le f_{\rm shot} \le 156$ MHz. Gravitational accretion of neutrinos in the solar system would increase the frequency further, scaling with the cube root of the particle density. Moreover, the increased quantum nature of the neutrino liquid further justifies the simple model we have used.

The central value estimate in Eq. (10) assumes that all neutrinos contribute to the correlation effect. However, if only half of neutrinos participate in the correlated neutrino dynamics, as suggested by Fig. 6, then the central frequency would be reduced by a factor of $1/\sqrt[3]{2}$. For $\delta N_\nu = 0$ and $v_{\rm rel} = 369$ km/s this corresponds to 111 MHz. On the other hand Fig. 7 provides in quantitative fashion an opportunity to evaluate how the fraction varies with neutrino density enhancement. Thus measurement of resonance frequency comprises information about the neutrino quantum liquid.

The key point in our consideration is that such a structured neutrino background noise raises the possibility of detection of the relic neutrinos via resonant amplification of the momentum transfer from neutrino scattering. We note that the peak at $f_{\rm shot} = 111$–140 MHz for $\delta N_\nu = 0$ and $v_{\rm rel} = 369$ km/s is in a domain where one could argue an accidental noise signature could have already been observed. This noise would arise from neutrino elastic scattering resonating with electromagnetic mechanical resonators. Given that there is a strong cosmic background in this frequency range, see e.g. Ref. [34], an exploration of the background noise signature has probably not been undertaken.[1] We thus believe that in the interesting frequency range the variation of in-detector observed noise as a function of terrestrial observer

[1] Bruce G. Elmegreen, private communication.

velocity vector with respect to the CMB is at present unexplored.

To better understand the noise spectrum, including the very important resonance peak width, a significantly more precise model of the CNB correlations is needed. We do not attempt to undertake this here. However, we believe that the distinct frequency of the impact correlation can vastly enhance the mechanical force when the effect is integrated over sufficiently long period of time and the detector has minimal damping.

6 Discussion

Remarks about dark matter: While very different in detail, a challenge similar to CNB detection exists with the effort at direct detection of dark matter. Provided that some physical property of dark matter correlates the temporal mechanical impacts, the here proposed resonant mechanical force detection method also applies to dark matter detection.

Considering a dark matter particle mass M_D, with lower limit of a few MeV [35], and the dark matter content in the Universe (20 % of all gravitating energy), one can estimate dark particle density. Assuming that a sizable fraction of dark matter impacts is correlated we find the impact frequency, f_D, is reduced to below MHz, and is decreasing as a function of mass, $f_D \propto M_D^{-1/3}$. The dark matter and neutrino signatures are thus well separated in frequency and both merit further experimental study by the here proposed novel resonant method.

Conclusions: In this work we have characterized the relic cosmic neutrino spectra in terms of their velocity, energy, and de Broglie wavelength distributions in a frame of reference moving relative to the neutrino background, with all examples focused on an Earth bound observer. We have shown explicitly the mass, m_ν, dependence and the dependence on neutrino reheating expressed by N_ν, choosing a range within the experimental constraints.

The dependence on N_ν and m_ν shown as a ratio on linear scale in Fig. 4 (bottom frame) is sufficiently strong to suggest that if and when relic neutrino detection becomes possible both N_ν and m_ν would be directly measurable. The effect of N_ν as presented here is to increase neutrino flux [18]; see Eq. (5). However, to this end one must gain precise control over the enhancement of neutrino galactic relic density due to gravitational effects [26] as well as the annual modulation [31].

As we argued in Sect. 4, the relic background of massive neutrinos will not behave as a purely free-streaming gas, but have properties of a quantum liquid. This inevitably leads to impact correlations which will cause the power spectrum due to neutrinos scattering off a detector to deviate from white noise, as we discuss in Sect. 5. The spectrum should exhibit a peak near a frequency arising from the relative velocity of the terrestrial observer with respect to CNB. Based on a simple model we find an expected range of 111–140 MHz for the central value, with the frequency increasing based on gravitational accretion enhanced neutrino density. The frequency is subject to modulation by the temporal variation of the observer velocity vector with respect to CNB. Such correlated structure in the noise spectrum opens the possibility for resonance based CNB detection methods, amplifying the otherwise negligible effect of neutrino drag.

Acknowledgments This work has been supported by US Department of Energy, Office of Science, Office of Nuclear Physics under award number DE-FG02-04ER41318 and was conducted with Government support under and awarded by DoD, Air Force Office of Scientific Research, National Defense Science and Engineering Graduate (NDSEG) Fellowship, 32 CFR 168a.

References

1. R. Opher, Astron. Astrophys. **37**, 135 (1974)
2. R.R. Lewis, Phys. Rev. D **21**, 663 (1980)
3. R. Opher, Astron. Astrophys. **108**, 1 (1982)
4. L. Stodolsky, Phys. Rev. Lett. **34**, 110 (1975) (erratum-ibid. 34, 508, 1975)
5. N. Cabibbo, L. Maiani, Phys. Lett. B **114**, 115 (1982)
6. B.F. Shvartsman, V.B. Braginsky, S.S. Gershtein, Ya.B. Zeldovich, M. Yu. Khlopov, JETP Lett. **36**, 277 (1982)
7. P. Langacker, J.P. Leveille, J. Sheiman, Phys. Rev. D **27**, 1228 (1983)
8. P.F. Smith, J.D. Lewin, Phys. Lett. **127A**, 185 (1983)
9. I. Ferreras, I. Wasserman, Phys. Rev. D **52**, 5459 (1995)
10. C. Hagmann, in Proceedings of the COSMO-98, edited by D. Caldwell (AIP, New York), vol. 478, 460 (1999)
11. G. Duda, G. Gelmini, S. Nussinov, Phys. Rev. D **64**, 122001 (2001)
12. G.B. Gelmini, Phys. Scripta **T121** (2005)
13. A. Ringwald, Nucl. Phys. A **827** (2009)
14. W. Liao, Phys. Rev. D **86**, 073011 (2012)
15. M.M. Hedman, JCAP **1309**, 029 (2013)
16. S. Betts et al., arXiv:1307.4738v2 [astro-ph.IM] (2013)
17. S. Weinberg, Phys. Rev. **128**(3), 1457 (1962)
18. J. Birrell, C.-T. Yang, P. Chen, J. Rafelski, Phys. Rev. D **89**, 023008 (2014)
19. G. Mangano, G. Miele, S. Pastor, T. Pinto, O. Pisanti, P.D. Serpico, Nucl. Phys. B **729**, 221 (2005)
20. Planck Collaboration, Planck 2013 results. XVI. Cosmological parameters. Astron. Astrophys. arXiv:1303.5076 (2014)
21. R.A. Battye, A. Moss, Phys. Rev. Lett. **112**, 051303 (2014)
22. K.A. Olive et al., Particle Data Group Collaboration. Chin. Phys. C **38**, 090001 (2014)
23. V.N. Aseev et al., Phys. Rev. D **84**, 112003 (2011)
24. Y. Choquet-Bruhat, *General Relativity and the Einstein Equations* (Oxford University Press, Oxford, 2009)
25. Y. Wong, Annu. Rev. Nucl. Part. Sci. **61**, 69 (2011)

26. A. Ringwald, Y.Y.Y. Wong, JCAP **0412**, 005 (2004)
27. G. Hinshaw et al., Astrophys. J. Suppl. **180**, 225 (2009)
28. G. Bertone, *Particle Dark Matter: Observations, Models and Searches* (Cambridge University Press, Cambridge, 2010)
29. M. Lisanti, B.R. Safdi, C.G. Tully, Phys. Rev. D **90**, 073006 (2014)
30. B. McElrath, Emergent Electroweak Gravity. arXiv:0812.2696
31. B.R. Safdi, M. Lisanti, J. Spitz, J.A. Formaggio, Phys. Rev. D **90**, 043001 (2014)
32. G. Kresse, J. Hafner, Phys. Rev. B **47**, 558 (1993)
33. E. Feenberg, Theory of Quantum Fluids. Academic Press, New York (1969)
34. S. Furlanetto, S.P. Oh, F. Briggs, Phys. Rep. **433**, 181 (2006)
35. C. Boehm, M.J. Dolan, C. McCabe, JCAP **1308**, 041 (2013). arXiv:1303.6270 [hep-ph]